fortune Journals

Research Article

ARCHIVES OF MICROBIOLOGY & IMMUNOLOGY

ISSN: 2572-9365



Nebulized Extended-Release Cationic PEGylated Nanoliposomal Delivery of Antiviral dual inhibitor MPI8 for Targeting SARS-CoV-2 Infection

Rama Kashikar[1], Shiqing Xu[2,3], Benjamin W Neuman[4,5], Wenshe Ray Liu[3,6], Pasupuleti Dedeepya[7,8], Sathish Kumar[4], Mahavir Bhupal Chougule[1]

Abstract

The purpose of the current research study was to encapsulate MPI8, a dual main protease (M^{Pro}) and host cathepsin L inhibitor in the nanoliposomal carrier along with the addition of PEG for stability and stealth properties and incorporation of coatsome-SS, a cationic lipid, for internalization of cells based on two pathways (MPI8-cSS-pegNL) and evaluate the lung disposition of nanoparticles following nebulization in an in-vitro model using the next-generation impactor. MPI8-cSS-pegNL suspension was prepared with MPI8, DPPC, Coatsome-SS, Cholesterol, and DOPE-PEG2000 using the ethanol injection method. MPI8-cSS-pegNL suspension was characterized for physical and aerosol properties. In vitro release studies were performed to determine the release kinetic profile. The particle size and entrapment efficiency of the MPI8-cSS-pegNL formulation were 180.5±2.6 nm and 95.479±1.842%w/v, respectively, after extrusion. The MPI8-cSS-pegNL released the drug in a controlled fashion for up to 12h, and in vitro aerosolization of the MPI8-cSS-pegNL formulation showed a mass median aerodynamic diameter (MMAD) of 4.40±0.24 µm, geometric standard deviation (GSD) of 2.02 ± 0.09, and fine particle fraction (FPF) of 37.88% ± 3.28. The MPI8-cSS-pegNL treatment for 48 h and 72 h showed antiviral efficacy against SARS-CoV-2.

Keywords: Main protease, Host cathepsin L inhibitor, Nanoliposomes, Nebulized, Antiviral

Introduction

Coronavirus disease 2019 (COVID-19) is a highly contagious infectious condition resulting from severe acute respiratory syndrome coronavirus 2 (SARS-CoV-2) infection [1]. After emerging in late 2019, the disease spread rapidly, leading to a global pandemic. SARS-CoV-2 belongs to the family of coronaviruses and is like SARS-CoV and MERS-CoV, the causative agents of the SARS and MERS pandemics of 2002-2003 and 2012-2013, respectively. SARS-CoV-2 is primarily spread through respiratory droplets in the nasal cavity and lungs and contact with contaminated surfaces [1]. The symptoms of SARS-CoV-2 infection are cough, fever, fatigue, and shortness of breath. Severe cases of infection can lead to pneumonia, acute respiratory distress syndrome, septic shock, and even death. The best way to prevent its spread is to practice good hygiene and social distancing [2]. SARS-CoV-2 is highly contagious, primarily transmitted through respiratory droplets or direct contact. Symptoms range from mild respiratory issues to pneumonia and acute respiratory distress syndrome [3]. Morbidity and mortality result from viral infection and the subsequent inflammatory response.

Affiliation:

[1]Indigenious Bioengineering and Drug and Gene Delivery (iBDG) Laboratory, Department of Pharmaceutical Sciences, Mercer University, Atlanta, GA, USA

[2]Department of Pharmaceutical Sciences, Irma Lerma Rangel College of Pharmacy, Texas A&M University, College Station, TX, 77843, USA

[3]Texas A&M Drug Discovery Center and Department of Chemistry, Texas A&M University, College Station, TX, 77843, USA

[4]Department of Biology, Texas A&M University, College Station, Texas, 77843, USA

[5]Department of Microbial Pathogenesis and Immunology, Texas A&M University, College Station, Texas, 77843, USA

[6]Institute of Biotechnology and Sciences and Department of Translational Medical Sciences, Texas A&M University, Houston, TX, 77030, USA

[7]Vaccine Nanotechnology Laboratory, College of Pharmacy, Center for Drug Delivery Research, Mercer University, Atlanta, GA 30341, USA

[8]Department of Pharmaceutical Sciences, College of Pharmacy, Larkin University, Miami, FL 33169, USA

***Corresponding author:**
Mahavir Bhupal Chougule, Department of Pharmaceutical Sciences, Mercer University College of Pharmacy, Atlanta, GA 30341, USA.

Citation: Rama Kashikar, Shiqing Xu, Benjamin W Neuman, Wenshe Ray Liu, Pasupuleti Dedeepya,, Sathish Kumar, Mahavir Bhupal Chougule. Nebulized Extended-Release Cationic PEGylated Nanoliposomal Delivery of Antiviral dual inhibitor MPI8 for Targeting SARS-CoV-2 Infection. Archives of Microbiology and Immunology. 10 (2026): 156-169.

Received: May 12, 2026
Accepted: May 18, 2026
Published: October 05, 2026

Kashikar R, et al., Arch Microbiol Immunology 2026
DOI:10.26502/ami.936500249

Several vaccines and therapeutics have been approved or authorized in the United States for the prevention and treatment of COVID-19 [4, 5]. Among vaccines, the Comirnaty and Spikevax (both mRNA-based) and the protein subunit vaccine Nuvaxovid have received FDA approval for use in specific populations. The FDA-approved antivirals Veklury and Paxlovid, as well as additional therapies such as Lagevrio and immunomodulators such as Actemra, Olumiant, Kineret, and Gohibic, are under Emergency Use Authorization for specific clinical scenarios [6]. However, there are limitations to each in cases where a patient presents with severe disease, necessitating alternative treatments. Despite the availability of FDA-approved vaccines [7], including Spikevax and Nuvaxovid, annual booster vaccination rates remain very low, and the risk of infection persists. In the development of new medicines, nanoparticle-based therapies have shown promising results against COVID-19 [8]. FDA-approved ARIKAYCE nebulized, safer, endogenous lipid-based nanoliposomes (NLs) demonstrated efficacy and safety in *Mycobacterium avium* infection [9], thereby strongly supporting the translational potential of nebulized NLs for nasal or lung diseases. Synthetic polymers, silica, and metallic materials, due to their toxicity, impede their use in inhalation delivery for the treatment of inflammatory diseases. Currently, no delivery systems exist for administering SARS-CoV-2 antiviral drugs directly to the lungs, a crucial approach for combating severe forms of COVID-19 characterized by respiratory distress and pneumonia. Research is ongoing globally to develop effective vaccines and drugs, including conventional therapies and emerging approaches such as nanomedicine, due to the lack of previously approved, effective drugs against the CoV family [10, 11].

Additionally, novel monoclonal antibodies (mAbs) like 19-77 are being developed to neutralize emerging variants, and broad-spectrum antivirals (BSAs) are a high priority. The FDA's Vaccines and Related Biological Products Advisory Committee recommended a monovalent JN.1-lineage vaccine composition for 2025-2026, with updated mRNA vaccines (Moderna's Spikevax and mNexspike, Pfizer/BioNTech's Comirnaty) and protein-based vaccines (Novavax's Nuvaxovid) targeting the LP.8.1 variant. Despite these advancements, challenges remain, including the continuous emergence of resistant SARS-CoV-2 variants, limited treatment windows, and unequal access to therapies. The RECOVER Initiative continues to conduct research on Long COVID, with several treatment strategies in development and clinical trials ongoing through 2026. There is an unmet need for new investigations and treatments that focus on direct lung delivery of antiviral drugs to improve COVID-19 outcomes with improved safety profiles. Nanomedicine offers a promising avenue to address limitations of traditional antiviral drugs, such as solubility and toxicity, and can enhance the potency and selectivity of antivirals against viral cells [10]. There is a continuous need for new medications, given that the current understanding of COVID-19 and its vulnerabilities has not fully translated into approved standard treatments, and the virus can lead to severe conditions like acute respiratory distress syndrome and multi-organ failure. The development of new antiviral treatments and preventive therapies is an active part of ongoing drug development [12]. Encapsulated ivermectin in orally administrable nanoparticles reduced the expression of the viral spike protein and the angiotensin-converting enzyme 2 (ACE2) receptor, offering a potential multilevel inhibition mechanism against SARS-CoV-2 [13].

Inhaled nanomedicine is a promising strategy for the prevention and treatment of COVID-19 by delivering therapeutic agents directly to the nasal passages or lungs, i.e., the site of infection [14]. This approach overcomes limitations of conventional antiviral therapies, such as poor solubility and systemic side effects, by targeting the lungs, where the virus primarily impacts [15]. Nanoparticles can enhance drug solubility, stability, and efficacy, facilitate extended-release, and mimic viral characteristics to effectively interact with viral proteins, thereby improving therapeutic outcomes and offering novel strategies [16]. The significance of inhaled therapeutic agent-loaded nanomedicine in the management of viral infections lies in its ability to block receptor binding and viral replication, and to improve pharmacokinetics and pharmacodynamics [17]. In vaccine development, it plays a crucial role, particularly for protein constructs and nucleic acid-based vaccines, stabilizing antigens and boosting immune responses. Nanomedicine provides broad-spectrum potential against various viruses, including coronaviruses, making it a valuable tool for addressing current and future pandemics. Among the inhaled devices, the nebulizers are self-administrable, easy to use, and allow for the delivery of large doses, making them suitable for both ambulatory and critically ill patients.

For the first time, we are exploring a new chemical entity: a dual inhibitor of the main protease (M^{Pro}) and host cathepsin L for the treatment of SARS-CoV-2 infection. Our investigation using antiviral drug Camostat mesylate-loaded nebulized nanoliposomes demonstrated that the formulation meets its target profile and the requirements of inhalation delivery systems [18, 19] and shows antiviral effects against viral infection.

For the treatment of COVID-19, multiple M^{Pro} inhibitors with no definitively identified selectivity have been screened [20]. A peptide aldehyde inhibitor of SARS-CoV-2, MPI8, displayed high antiviral and cathepsin L inhibition properties. Cathepsin L, TMPRSS2, and furin are responsible for SARS-CoV-2 entry into host cells and for its replication [20]. Ma and the group have shown that MPI8 has high potential to

Citation: Rama Kashikar, Shiqing Xu, Benjamin W Neuman, Wenshe Ray Liu, Pasupuleti Dedeepya,, Sathish Kumar, Mahavir Bhupal Chougule. Nebulized Extended-Release Cationic PEGylated Nanoliposomal Delivery of Antiviral dual inhibitor MPI8 for Targeting SARS-CoV-2 Infection. Archives of Microbiology and Immunology. 10 (2026): 156-169.

Kashikar R, et al., Arch Microbiol Immunology 2026
DOI:10.26502/ami.936500249

simultaneously and selectively inhibit M^{Pro} and host cathepsin L, demonstrating its potential as a highly potent antiviral drug [20].

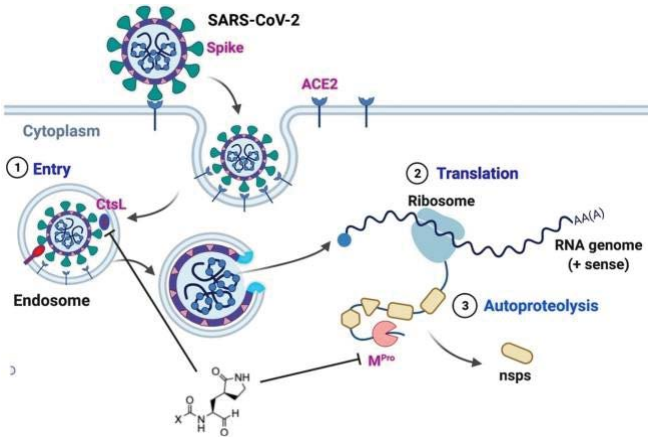


Figure 1: Mechanism of MPI8 to inhibit the M^{Pro} and the host Cathepsin L to prevent the replication of virus in the human cell. The figure shows a peptide aldehyde inhibitor mechanism in inhibiting both the M^{Pro} in the viral cells and Cathepsin L receptor in the host cell to inhibit the replication of virus and prevent the progression of COVID-19 disease.

Based on the above findings, we hypothesized that the formulation of inhalable, extended-release, nebulized MPI8-loaded endogenous lipid-based nanoliposomes will provide an effective therapeutic window in the lungs without the need for invasive procedures. The drug will inhibit the virus's TMPRSS2-mediated infection and the host Cathepsin L, thereby treating COVID-19 (Figure 1). The objectives of this study were to develop inhalable, extended-release, nebulized MPI8-loaded nanoliposomes with an ionizable lipid to aid drug internalization (MPI8-cSS-pegNLs) and to evaluate them using physicochemical and in vitro methods, such as size, zeta potential, entrapment, stability, release profile, and aerodynamic performance using the next-generation impactor, and antiviral efficacy against SARS-CoV-2.

Materials and Methods

Materials

1,2-dipalmitoyl-sn-glycerol-3-phosphocholine (DPPC- Lot# G160PC-62) and 1,2-dioleoyl-sn-glycerol-3-phosphoethanolamine (DOPE-PEG- Lot# 880130-01-049) were purchased from Avanti Polar Lipids Inc. (Alabama, USA). Cholesterol (Lot# 0786C157) was purchased from VWR Life Sciences (Bridgeport, NJ, USA). Cationic Lipid Coatsome SS-OP (Lot# M21N611) was purchased from NOF Corporation (White Plains, NY, USA). Sodium chloride (Lot# Z76929) was obtained from Research Organics (Cleveland, OH, USA). Ethanol (Lot # 2701) was purchased from Decon Laboratories (Philadelphia, USA). MPI8 was obtained from our collaborators at Texas A&M University, TX, USA. Other chemicals and materials required for the project, such as HPLC-grade solvents, centrifuge tubes, HPLC vials, and scintillation vials, were obtained from Fisher Scientific (Hampton, NH, USA).

Methods

Formulation development

Based on our previous study on the development of liposomes using a quality-by-design approach, we optimized the excipients and process parameters for the formulation using the established ethanol injection method; the process is depicted in Figure 2A-B [18, 19].

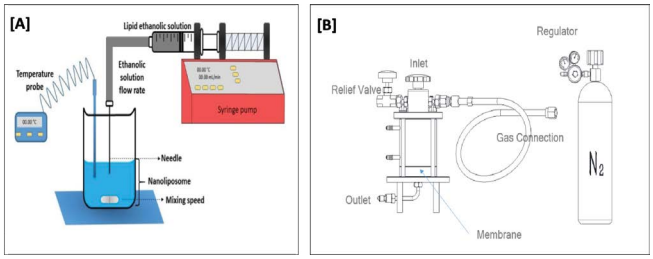


Figure 2: [A] This figure depicts a schematic representation of the ethanol injection method for formulation of the nanoliposomal suspension. The syringe pump maintains the flow rate at 0.1mL/min, while the temperature is maintained at 55°C, and stirring is continuous for 30 minutes after complete incorporation of the lipids into the aqueous phase. [B] This figure is a schematic representation of the extruder setup. It is a jacketed vessel that maintains the temperature at 55°C while the entire contents of the formulation pass through a 0.1µm membrane under 200-300 psi pressure generated by the nitrogen gas.

We used 12.5 mg of the drug in 10 mL of formulation, based on the IC50 value reported by our collaborator, Dr. Liu's group [20]. We used 4.322 mg of DPPC, 4.322 mg of coatsome-SS ionizable lipid, 3.232 mg of cholesterol, and 2 mg of DOPE-PEG2000, which we dissolved in 0.67 mL of 90% v/v ethanol. We used 10 mL of 0.9% w/v NaCl solution as the aqueous phase (Table 2). We maintained the temperatures of both the aqueous and ethanolic phases at 55°C, which was just above the glass-transition temperature of all lipids in each phase. Using a flow rate of 0.15 mL/min on a syringe pump (New Era Pump System Inc., Model# 300) with a 5 mL glass syringe with a narrow orifice (10.3 mm) and a constant stirring speed of 600 rpm, we incorporated the ethanolic phases into the aqueous phase, yielding a nanoliposomal suspension. We maintained the temperature and stirring speed for up to 30 min after complete incorporation of lipids into the aqueous phase using a magnetic hot plate (IKA® C-MAG HS 7 - control).

This yielded a particle size larger than desired, so we used a Genizer jacketed mini extruder with a 0.1 µm membrane. For the extrusion process, we poured the entire formulation

Kashikar R, et al., Arch Microbiol Immunology 2026
DOI:10.26502/ami.936500249

Table 1: Component values used to formulate the MPI8-cSS-pegNLs. The values were obtained from the QbD design from a previous study. The drug concentration is based on the drug's IC_50 value.

Ingredient	Quantity
MP18	6.25mg
DPPC	4.32mg
Coatsome-SS	4.32mg
DOPE-PEG	1mg
Cholesterol	3.43mg
Ethanol	0.65mL
Sodium Chloride	90mg
20 mM malic acid (pH 4.0) in water	QS 10mL

into a jacketed vessel maintained at 55°C with a 0.1µm membrane at the bottom. We closed the vessel's top lid, started the nitrogen gas, and allowed it to reach 200-300 psi. The formulation passes through the filter dropwise, and the filtrate is collected in an amber-colored vial. After finishing, we open the exhaust to reduce pressure inside the vessel, then open the vessel and check for any drug deposits on the filter and the membrane's integrity. At the end of the experiment, we clean the vessel and allow it to air dry. The formulation was then dialyzed for 5h using 500mL of 0.9% w/v NaCl and 50 kDa dialysis bags, maintaining the temperature at 37°C.

Characterization of formulated MPI8-cSS-pegNL using the Malvern Zetasizer

Using the Malvern Zetasizer, we employed Dynamic Light Scattering (DLS) to measure the particle size of the globules formed and their polydispersity index, which reflects the homogeneous or heterogeneous distribution of the formulated nanoparticles in the vehicle, as described previously [18, 19]. To measure particle size and polydispersity index, we used a disposable folded cuvette with a capacity of 1 mL, containing 100 µL of the sample. Along with the measurement of the particle size and particle size distribution, also called polydispersity index (PDI), we measured the surface charge of the formulated nanoliposomes to understand if the particles were stable in the suspension form [18, 19]. To measure the zeta potential, we used zeta cells with conductor rods in the cell to conduct charge when placed in the zeta sizer, and the current is applied. We used 700 µL of the sample to measure zeta potential.

LC-MS method development for chemical characterization

To determine drug percentage in subsequent studies, including chemical characterization of % entrapment efficiency, % drug loading, and % assay, we developed an LC-MS method. For method development, we noted that the compound's molecular weight is 601 Da [21]. Using an Agilent triple-quad mass spectrometer, we developed a method to characterize MPI8. Initially, to determine the retention times of the molecule and its fragments, we performed a total ion scan using a mobile phase of 0.1% formic acid in water: 0.1% Methanol (25:75, isocratic). We used Antipyrine with a molecular weight of 189 Da as an internal standard. We used a Luna®3um C18(2) 100ÅLC Column 50x3mm for the characterization, which was maintained at 30°C throughout the run. For this method, we used a flow rate of 0.5 mL/min and an injection volume of 5 µL. We observed that the retention time of the internal standard, Antipyrine, was about 0.83 min, while that of MPI8 was 1.83 min. After generating a standard curve using the TIC, we developed an MRM method to identify the ion. MPI8, with a molecular weight of 601.3 Da, splits into two ions at 545.3 Da and 157.2 Da (Table 1). We used the 157.2 Da fragment of the parent molecule for further quantification. The process parameters for the MRM method development remained the same, except for a few additions noted above.

Determination of entrapment efficiency, drug load, and assay of MPI8-cSS-pegNLs

The free drug determination technique for the characterization of the entrapped and loaded MPI8 in the MPI8-cSS-pegNLs was used. For this, we used 10kD Amicon filters. We added 300 µL of the formulation nanosuspension to the Amicon filters and centrifuged them for 15 min at 13000 rpm. The filtrate collected in the tube was diluted with the mobile phase without 0.1% formic acid to ensure that the MPI8 concentration was within the linearity range. We put the samples into vials and analyzed them using the LC-MS method, as described earlier. We used the following formulae to calculate the amount of entrapped drugs and the drug loading of MPI8 in the MPI8-cSS-pegNLs.

Table 2: Parameters used in the method development and further characterization of MPI8. Source parameters such as Gas Temperature, Gas Flow, Nebulizer, and capillary positive voltage were maintained at 300°C, 11 L/min, 15 psi, and 4500V, respectively.

Precursor Ion	Product Ion	Dwell	Fragmentor	Collision Energy	Cell Accelatator Voltage	Polarity
601.3	157.2	200	135	30	7	Positive
601.3	545.3	200	135	20	7	Positive
189	131	200	135	28	7	Positive

Citation: Rama Kashikar, Shiqing Xu, Benjamin W Neuman, Wenshe Ray Liu, Pasupuleti Dedeepya,, Sathish Kumar, Mahavir Bhupal Chougule. Nebulized Extended-Release Cationic PEGylated Nanoliposomal Delivery of Antiviral dual inhibitor MPI8 for Targeting SARS-CoV-2 Infection. Archives of Microbiology and Immunology. 10 (2026): 156-169.

Kashikar R, et al., Arch Microbiol Immunology 2026
DOI:10.26502/ami.936500249

Equation 3:% $Assay = \frac{Amount\ of\ drug\ obtained\ (\frac{mg}{mL})}{Theoretical\ ampunt\ of\ drug\ (\frac{mg}{mL})} \times 100$

For the determination of the % assay for MPI8 in MPI8-cSS-peg-NLs

We used 500 µL of the formulation, adding 250 µL of methanol and 250 µL of 50% Triton-X100. We sonicated this solution for an hour in a bath sonicator. Once you observe a cloudy precipitate, centrifuge the tube at 13000 rpm for 15 min. We collected the supernatant from which the drug was extracted, then diluted it with the mobile phase without 0.1% formic acid to ensure MPI8 remained within the established linearity range. The samples were then analyzed using the developed LC-MS method. We analyzed the collected data using Agilent qualitative and quantitative software, followed by using this formula to obtain the % assay of MPI8 obtained from MPI8-cSS-pegNLs.

Equation 3:% $Assay = \frac{Amount\ of\ drug\ obtained\ (\frac{mg}{mL})}{Theoretical\ ampunt\ of\ drug\ (\frac{mg}{mL})} \times 100$

In-vitro drug release study

This study intends to understand the release profile of the MPI8-cSS-pegNLs. Our discretion for this nanoliposome suspension is twice-daily delivery of the formulation via nebulization. Twice-daily delivery is generally patient-compliant among adults, pediatric, and geriatric patients.

For this study, we prepared six vials: three control solutions and three MPI8-cSS-pegNLs. We prepared the control solution by dissolving the drug in 70% ethanol, as it is lipophilic. We took 20mL of release media, which was simulated lung fluid (Figure 3). We soaked the float-a-lyzer membranes, which were 100kD in molecular weight, which was 175 times the molecular weight of MPI8 in the SLF, and maintained 37°C overnight to help saturate the membrane with the surrounding media and open the pores on the membranes enough to help with the release of the drug at 37°C, 1 mL. During the study, we aliquoted 1mL of the SLF at each predetermined time point and replaced it with fresh medium to maintain the volume. The collected samples were diluted to fit into the linearity range using the mobile phase and analyzed using the developed LC-MS method. For the calculation, we considered the cumulative release and plotted it against the time points at which we aliquoted, in hours. The release profile was analyzed using DDSolver software.

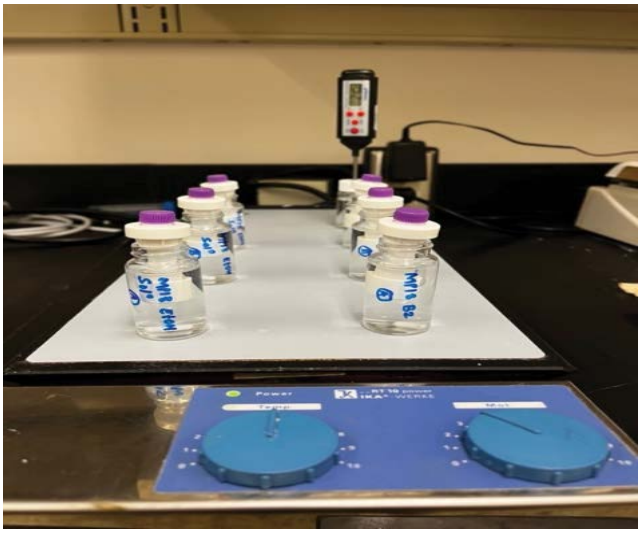


Figure 3: This figure depicts the in vitro release study setup. We had 3 control and 3 MPI8-cSS-pegNL vials. The temperature of the vials was maintained at 37°C throughout the experiment. Aliquots were taken at 0.5h, 1h, 2h, 4h, 8h, 12h, 24h.

Aerodynamic Characterization Study

Principle of Cascade Impactor:

The arrangement of plates in a series is the primary layout of the Next Generation Impactor. As we proceed, the diameter cut-offs on each plate decrease, increasing airflow through the smaller orifice. The smaller and, in turn, lighter particles will float in the air stream longer before they hit the collection plate. The particles will hit the plate if they can no longer float in the air[22] (Figure 4A-B). Performing this analysis is essential, as it provides a direct relationship between the mass of active pharmaceutical ingredients and aerodynamic particle size, which is regarded as an indicator of the anticipated deposition site within the respiratory tract.

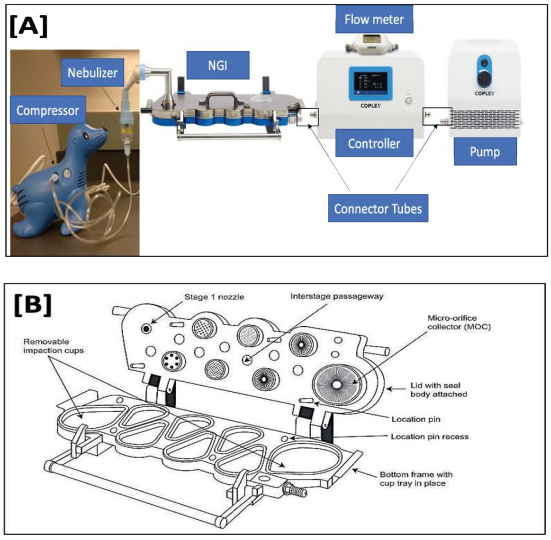


Figure 4: **[A]**This figure depicts the entire setup of the next-generation impactor used for the aerodynamic characterization of the nanoliposomal suspension after nebulization. The nebulized nanoliposomes are pulled into the induction port and flow through the impactor at a specified flow rate of 30±0.5 L/min. **[B]** This diagram is a schematic representation of the various stages inside the next-generation impactor. The nebulized particles flow through the impactor and deposit on the respective stages based on their particle sizes.

Kashikar R, et al., Arch Microbiol Immunology 2026
DOI:10.26502/ami.936500249

There are eight stages, including the micro-orifice collector (MOC) stage. Additionally, a filter paper is placed at the bottom of the filter stage [18, 19]. We weighed each cup before coating the plates with the surfactant and recorded the weights as the plates' tare weights pre-run. Following this, we coated each plate on the stage with a nonreactive surfactant, poloxamer 188. Coating the cups was essential to prevent particle bounce at high flow rates during the study. We applied an even, thin film of poloxamer 188 to each plate and weighed the cups again. We recorded the cups' gross weights pre-run. Once coated, we weighed the filter paper and placed it at the bottom of the filter stage. Then, we carefully placed each cup on the stage, arranging them from cup 1 through MOC from left to right. The left stage, or stage 1, is attached to the induction port. We then weighed the mouthpiece pre-run and recorded the tare and gross weights. Since no coating was applied to the mouthpiece, the tare and gross weights pre-run remained the same.

Consequently, we weighed the empty nebulizer and recorded that weight as a pre-run tare weight. We added the 5mL of the prepared solution to the nebulizer, weighed it again, and recorded the weight as the nebulizer's pre-run gross weight. Subtracting the nebulizer's pre-run tare weight from the nebulizer's pre-run gross weight, we can calculate the weight of the solution added to the nebulizer. The solution weight added to the nebulizer is required to calculate the Mass Median Aerodynamic Diameter (MMAD), Geometric Standard Deviation (GSD), and percent Fine Particle Fraction (%FPF). We attached the filled nebulizer to the mouthpiece at the ACI's induction port. We used Sami, the seal for the nebulization. The final setup of the instrument was achieved, as shown in the figure (Figure 4A). The nebulizer and pump are operated for 10 minutes at a flow rate of 30±0.5 L/min, as prescribed in the United States Pharmacopeia (USP). After the experiment, we disassembled the system in reverse order. We weighed the nebulizer with the remaining solution and recorded the combined weight as the post-run gross weight. We weighed the mouthpiece, all the cups, and the filter paper, and recorded their post-run gross weights. We performed n=3 runs to determine the reproducibility of the parameters using the NGI.

Evaluation of the antiviral effect of MPI8-cSS-pegNL

SARS-CoV-2 variant BQ.1.1 was cultured on VERO E6-ACE2-TMPRSS2 cells. Cells were inoculated at a multiplicity of 0.1 TCID50 units per cell and incubated for 1h to allow for virus adsorption, rinsed three times with phosphate-buffered saline to remove unbound inoculum, and treated by the addition of DMEM culture medium supplemented with 10% fetal bovine serum, 1x antibiotic antimycotic, and the desired concentration of dissolved or nanoliposome-loaded drugs, with four replicates per datapoint. Aliquots of medium were collected 48h and 72h after inoculation, and the amount of virus genomes in the supernatant was quantified using a Luna One-Step RT175 qPCR assay (New England Biolabs), with the N1 primer and probe set, calibrated against a standard curve of inactivated viral RNA (BEI Resources, NR-52285). EC50 values were calculated from the part of a dose-response series showing a log-linear effect.

Results and Discussion

Development of MPI8-cSS-pegNL

For the development of nanoparticles, we weighed the excipients based on previous research from our lab on a TMPRSS2 inhibitor[18, 19]. The primary difference between the previously developed formulation and the current formulation is that the current formulation is intended for endosomal delivery to the cytosol by rupturing the endosomal membrane. The cationic, ionizable lipid facilitates that function [23]. Another reason for the use of the cationic lipid is that it plays a critical role in endosomal uptake with two mechanisms. The cationic lipid might interact directly with the negative charge on the cell membrane or bind to a plasma protein that facilitates cellular uptake. In addition, ionizable lipids increase encapsulation efficiency to above 90% [23]. Due to these attributes, we used a 50% w/w concentration of the cationic, ionizable lipid in our formulation. DPPC is an endogenous lung phospholipid that forms a phospholipid bilayer. DPPC is an endogenous lipid found in ample quantities in lung fluid, making it a suitable lipid for the local delivery of these developed products to the lungs. The cholesterol in this formulation provides the phospholipid bilayer with sufficient rigidity to prevent the contents entrapped within it from leaking. The DOPE-PEG2000, another endogenously available component, provides stealth characteristics by coating the nanoparticles in the formulation. The volume of nanoparticles in the formulation was determined based on a study by Gouda Ahmed and team on the ethanol injection technique, which explains the factors influencing the technique, the challenges, and its application [24]. The concentrations of components other than the ionizable lipid were derived using a quality-by-design approach applied to a similar formulation in our previous research [19].

Numerous nanoparticle-based therapies and vaccines for COVID-19 are in various stages of clinical trials. Nanoparticles offer several therapeutic strategies, including blocking viral entry, inhibiting replication, and directly inactivating the virus. Our lab has demonstrated that the antiviral camostat mesylate-loaded extended-release nebulized nanoliposomes were effective against SARS-CoV-2 infection [18, 19]. Chloroquine, when encapsulated in polymeric nanoparticles like poly(lactic acid) (PLA), can effectively block the endocytosis of SARS-CoV-2 particles [25]. Cationic carbon dots (CDs) derived from curcumin have been shown to block viral entry of coronaviruses like porcine epidemic diarrhea

Kashikar R, et al., Arch Microbiol Immunology 2026
DOI:10.26502/ami.936500249

virus (PEDV) by electrostatic interactions and also suppress reactive oxygen species (ROS) accumulation[25]. AgNPs, including those modified with curcumin, have demonstrated the ability to inhibit the entry of respiratory viruses into cells, with smaller particles often being more effective and less cytotoxic. Gold nanorods functionalized with peptides can block the formation of six-helix bundles, thereby inhibiting cell fusion and viral entry, as demonstrated with MERS-CoV [26]. Furthermore, certain nanoparticles, such as MUS: OT-AuNPs, can induce irreversible viral inactivation by deforming viruses, providing a broad-spectrum viricidal treatment against various human-infecting viruses [27]. Iron oxide nanozymes (IONzymes) can catalytically inactivate influenza A viruses (IAVs) by inducing lipid peroxidation in the viral envelope and destroying surface proteins [28]. Studies also indicate that multifunctional alveolar macrophage-like nanoparticles can act as decoys to block coronavirus entry into host cells and absorb pro-inflammatory cytokines, thereby achieving combined antiviral and anti-inflammatory effects. Encapsulated silymarin combined with curcumin significantly reduced interleukin-6 and C-reactive protein levels to 64 ± 0.8 Pg/μL and 6 ± 0.5 μg/μL, respectively, outperforming other treatments [29]. This formulation also demonstrated antiviral activity against COVID-19 in vitro and improved histopathological profiles, suggesting its potential as a muco-inhalable delivery system for combating inflammation and COVID-19.

Nanomedicine has been crucial to the rapid development of COVID-19 vaccines, particularly through the use of lipid nanoparticles (LNPs) for mRNA vaccine delivery. LNPs encapsulate mRNA, protecting it from degradation and facilitating its delivery to the cytoplasm, where it can be translated into target proteins to trigger immune responses [30]. The FDA has granted Authorization to several COVID-19 lipid nanoparticle vaccines, including mRNA-1273 (Moderna) and BNT162b2 (Pfizer-BioNTech). These mRNA-LNP vaccines have shown high efficacy and have played a pivotal role in global immunization efforts. LNPs are designed to maximize antigen presentation and enhance immune stimulation, leading to potent humoral and cellular immune responses. Research is also ongoing into self-amplifying RNA (saRNA) encapsulated in LNPs, such as LNP-nCoVsaRNA, which can induce robust antibody and cellular responses at lower doses [30].

Nanoparticle-based strategies against COVID-19 have been studied by our group and other researchers and applied across diagnostics, therapeutics, and vaccine development, leveraging their unique physicochemical properties, including size, surface charge, and functionalization. The advancements in nanomedicine during the pandemic have led to a rapid expansion of nanoparticle use in clinical settings, with a notable increase in clinical trials and approvals for nanoparticle-based products. Specifically, lipid nanoparticles (LNPs) have revolutionized mRNA vaccine delivery by protecting the mRNA cargo and facilitating its cellular uptake, as exemplified by the Moderna and Pfizer-BioNTech COVID-19 vaccines [31]. These vaccines, administered intramuscularly in two doses, encode for the SARS-CoV-2 spike glycoprotein, prompting an immune response. Beyond vaccines, nanoparticles are being investigated for intranasal delivery to directly target respiratory infections, with studies exploring silver and gold nanoparticles for their antiviral effects and ability to stimulate immune responses [32]. While intramuscular administration is the primary route for many COVID-19 nanovaccines, intranasal delivery offers benefits, including bypassing enzymatic degradation and enhancing drug action at mucosal surfaces. However, more research is needed for human application.

Characterization of the formulated MPI8-cSS-pegNL suspension

Particle size, polydispersity index, and zeta potential

The formulated nano liposomal suspension had a slightly higher particle size than we desired. Our target particle size for the developed nanoparticle was <250nm. The initial particle size we observed was about 292.5±6.6 nm. So, we proceeded with the extrusion, which reduced the particle size to 180.5±2.6 nm (Figure 5). Based on prior literature, an article by Nahar Kamrun and colleagues on enhancing site-specific vasodilation in pulmonary hypertension using a peptide-coated liposomal formulation of fasudil is also consistent with our results. They made their liposomes using DPPC, DSPC, DSPE, and DOPE. They used a thin-film hydration technique to formulate their nanoliposomes, yielding a particle size slightly higher than their desired size, which was achieved by extrusion through an extruder. Liposomes were prepared using 50 μmol lipids, including DPPC, cholesterol, and DSPE-PEG2000. Different formulations were prepared by adding DSPE, DSPE-Mal2000, DPPE, or DOPE as the fourth lipid, at a molar ratio of 70:30:5:5. These lipids were conjugated to the cysteine group of the CAR peptide.

The lipid mixture was dissolved in chloroform/methanol, forming a thin lipid film under vacuum. The film was rehydrated with 250 mM ammonium sulfate (pH 4.5), and liposomes were obtained through sonication and extrusion. Ammonium sulfate was replaced with PBS using a PD-10 column. Fasudil was encapsulated by creating an ammonium sulfate gradient, and liposomes were incubated with Fasudil before the unencapsulated drug was removed using a PD-10 column. The data coordinates with the data available in the literature. In another article by Sebaaly C et al., the researchers developed eugenol-loaded liposomes using an ethanol injection method. They employed a 2:1 phospholipid-to-cholesterol ratio, which was close to the ratio used in our

Kashikar R, et al., Arch Microbiol Immunology 2026
DOI:10.26502/ami.936500249

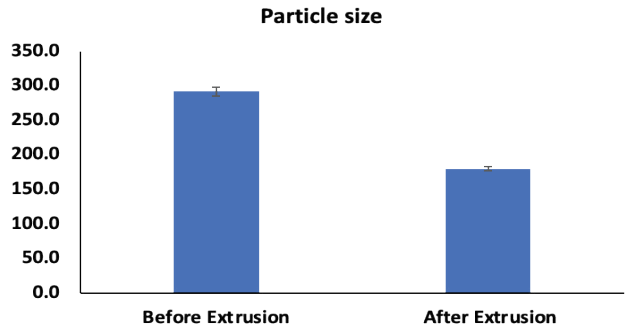


Figure 5: This figure depicts the difference between the particle size of MPI8-CSS-PEGNLs before and after the extrusion using the Genizer mini extruder. On passing the MPI8-cSS-pegNL through a 0.1µm membrane, a statistically significant decrease was observed in the reading. We ran a t-test to confirm that the difference was statistically significant and found a p-value < 0.05.

study [33]. Phospholipids and cholesterol were dissolved in absolute ethanol and injected into ultrapure water using a syringe pump. The injection occurred at a temperature above the transition temperature of the constituent phospholipids. For Phospholip 80H and Phospholi 90H, it was 55 °C, while for Lipoid S100, it was 25 °C. Liposomes form instantly upon mixing the organic and aqueous phases. The liposomal suspensions were stirred at room temperature for 15 minutes. Subsequently, rotary evaporation at 40 °C under reduced pressure removed ethanol and some water, and the liposomal suspension was stored at 4 °C [33]. They found the particle size to be higher, around 210±26nm, which was also our observation in our study.

The polydispersity index of the formulation was within the desired range prior to extrusion. However, after the extrusion process, the polydispersity index did not change drastically and remained within the desired range of <0.3, implying that the formulation is a monodisperse system [34]. It is essential to have a monodisperse phase for the formulation of safe, stable, and efficient nanoparticles [34]. We found the PDI of MPI8-cSS-pegNLs to be 0.144±0.028. This implies that it was a monodisperse nanoliposomal suspension, which would exhibit high stability and safety profiles. Our scientific findings were consistent with the published literature. Based on the literature, the liposomal formulation containing oleic acid and doxorubicin showed a PDI of around 0.15±0.03. The literature by Sarfraz M. et al. [32] describes a dual-drug-loaded liposomal formulation developed using a reengineered ethanolic injection method. Another research team, Thuan Thi Duong et al., studied a nanoformulation loaded with Berberine, comprising HSPC and DSPG, prepared via the ethanol injection method[35]. Upon characterization, the formulation had a PDI of about 0.11-0.25, which was consistent with the PDI observed for the MPI-cSS-pegNL.

The zeta potential of the formulation was measured using zeta cells and was found to be neutral to slightly positive. We reckon the slight positive charge is due to the addition of the cationic lipid. The PEG creates a hydration layer over the nanoparticles, which prevents biofouling and phagocytosis of the developed nanoparticles. Niven et al., in their study on pulmonary absorption of intratracheal and aerosolized formulations, observed that the nanoparticles had a prolonged pulmonary effect and were non-toxic. We found the zeta potential for MPI8-cSS-pegNLs to be 0.597 ± 0.038 mV. In a literature review by Mackensie Smith et al., a case study on liposomes with different charges reported the formulation of liposomes using DSPC, cholesterol, DOTAP, and DOPS. DOTAP was the cationic lipid used[36]. To formulate the liposomes, a thin-film hydration technique was used and characterized using the DLS technique based on a Malvern instrument. They found that the zeta potential of their formulation ranged from -10 mV to 10 mV [36], which was consistent with our findings. Another study with findings similar to ours was published by Tomomi Akita et al. on Am-80-encapsulated lipid nanoparticles containing Coatsome-SS-OP, which reported the formation of neutral nanoliposomes with a zeta potential of -4.07±1.54 mV. For the Am80-encapsulated liposomes, the authors formulated the product using the ethanol injection method, dissolving DOPE, DMG-PEG2000, Coatsome SS-OP, cholesterol, and the drug (Am80) in an ethanolic solution, which was then injected into a saline solution containing 20 mM malic acid [37].

Entrapment efficiency, drug load and assay

It is essential to determine the % entrapment efficiency to demonstrate that the MPI8-cSS-pegNLs contain no or negligible amounts of free MPI8. It is important that the developed nanoparticles are drug carriers intended to reach the target. Higher entrapment of MPI8 in the vesicles also implies a slower release of the drug compared to the free drug. As we aimed to develop a sustained-release nano liposomal suspension, our target was to achieve high entrapment efficiency. We found our % entrapment efficiency to be 60.773±2.681 % w/v before extrusion. We saw a significant increase in drug loading after extrusion. The % entrapment efficiency of the formulation increased to 95.479±1.842 % w/v (Figure 6). We hypothesize that this is the case because the liposomes are maintained at 55°C during extrusion, implying that the lipids in the formulation are at their glass transition temperature and, hence, moldable. Thus, they rearrange themselves and encapsulate more drugs during extrusion, after which, at room temperature, they solidify, resulting in higher drug encapsulation. Our results were in close agreement with the literature by Chiraz Jaafar-Maalej et al. on liposome preparation using the ethanol injection method for hydrophilic and lipophilic drugs [38]. The authors

Kashikar R, et al., Arch Microbiol Immunology 2026
DOI:10.26502/ami.936500249

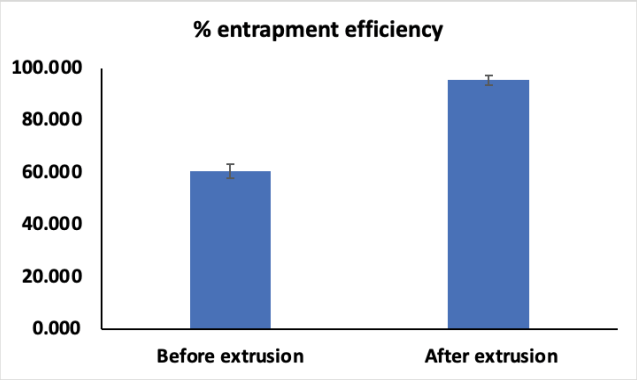


Figure 6: This figure depicts the difference between the % entrapment efficiency of the formulation before and after extrusion. The graph shows a statistically significant difference among the % entrapment efficiency values. Analyzed using a t-test to confirm the significance and found a p-value of < 0.05.

of this article state that lipophilic drugs achieve higher entrapment efficiency because they are dissolved in the lipid phase before being injected into the aqueous phase. They achieved 100% entrapment efficiency for the hydrophobic drug beclomethasone dipropionate [38]. Using another study by Tomomi Akita et al. on Am-80-encapsulated lipid nanoparticles, a high entrapment efficiency of 71.3±8.49 % w/v was observed. The authors employed the ethanol injection method to prepare liposomes entrapping Am80. Lipids, including cholesterol, coatsome SS-OP, DMG-PEG, and DOPE, were solubilized in ethanolic solution and injected into 0.9%w/v saline containing 20 mM malic acid [37].

For the % assay calculation, we accounted for free MPI8 and released entrapped MPI8 from the formulation by rupturing the membranes with Triton X-100, a detergent. Upon releasing the vesicles' contents, we expect the assay values to be close to 100%. On analysis and calculation using LC-MS, we found the formulation to be 100±0.236 % w/v. This was in line with our hypothesis. The extrusion process did not change the assay percentage, confirming no loss of drug to the membrane during extrusion. This implied that extrusion was a suitable process for reducing the particle size of the formulation without adversely affecting other parameters.

We also analyzed the MPI8-cSS-pegNL for % drug loading. % drug loading is the amount of drug available per mg of the vesicle. We found the MPI8-cSS-pegNL to have a high drug load of 62.170±0.741%w/w. A higher drug load is an important parameter because it implies a lower dose for patients. This implies that fewer excipients will have any adverse interaction or effect on the formulation. This implies a higher safety profile of the formulation. Extrusion did not have a significant effect on the formulation's % drug loading. Another study by Sarfraz M et al. reported a higher drug-loading efficiency of 91.67% for oleic acid [39]. A higher entrapment was observed because oleic acid is lipophilic and was entrapped in the lipid phase. The optimized formulation consisted of HSPC: cholesterol: DSPE-PEG2000 in a molar ratio of 64:31:5. A marked reduction in the loading of the hydrophilic compound Doxorubicin was observed. The thin-film hydration method was employed to formulate dual-loaded nanoliposomes containing oleic acid and doxorubicin [39].

In-vitro release study

The release studies were conducted under sink conditions, considering that a non-sink situation could substantially underestimate the drug release from nanoliposomes. Hence, the solubilities of the drugs in their respective release media were determined before the release study [40]. We have illustrated the release profiles of MPI8-solution and MPI8-cSS-pegNLs in the figure 7. A paired t-test was applied to statistically compare the release profiles of MPI8-solution and MPI8-cSS-pegNLs in PBS and in intracellular concentrations of glutathione (10 mM) at each time point. We found the *p-value* to be greater than 0.05 from the 0-hour time point because the release was 0% at the beginning of the study (Figure 7). All time points after that, up to 8 hours, showed a significant difference, as indicated by p-values < 0.05. At the 12-hour time point, MPI8-cSS-pegNL released 104.084±1.836% in the release media containing IC levels of GSH, so the p-value was > 0.05; however, a significant difference was observed between MPI8-solution and PBS

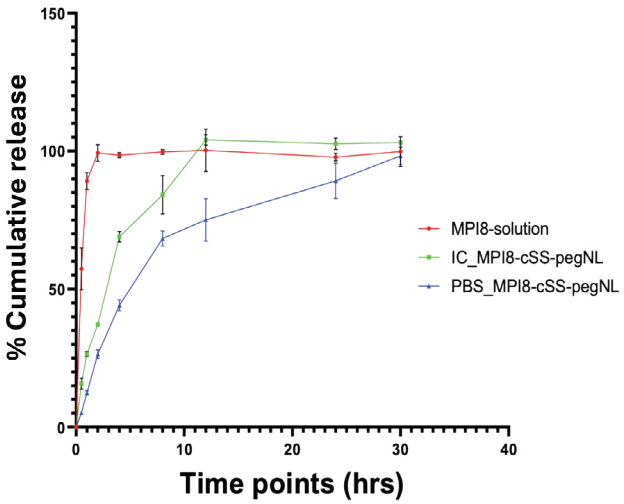


Figure 7: This figure depicts the release of the MPI8-control solution and MPI8-cSS-pegNLs. It is observed that the MPI8 follows a Korsmeyer-Peppas release model with and r^2 of 0.995 obtained from DDSolver. There was a statistically significant difference between time points at 1 hour, 2 hours, 4 hours and 8 hours of release. The formulation releases 104.084±1.836% of MPI8 in the first 12 hours, implying a requirement for twice-daily dosing.

Kashikar R, et al., Arch Microbiol Immunology 2026
DOI:10.26502/ami.936500249

($p<0.05$) and between the IC_{50} of MPI8-cSS-pegNL and PBS ($p<0.05$). At the 24-hour time point, the PBS_MPI8-cSS-pegNL also released 89.21±6.42% of the drug in PBS. We observed a statistically significant difference (p-value < 0.05) at 1, 2, 4, and 8 hours. The release is sustained for 12 hours, which is close to our target profile of twice-daily dosing.

In agreement with our findings, the Sabeti et al. research article discussed the development and characterization of doxorubicin hydrochloride-loaded nanoliposomes, which showed extended release of the drug. In vitro, the release of Doxorubicin hydrochloride from a liposome composed of Doxorubicin hydrochloride, palm oil, cholesterol (CH), L-alpha-phosphatidylcholine (PC), polyethylene glycol (PEG), methanol, and chloroform for 96 hours demonstrated a constant and continuous release profile. Within the first 12 hours, these liposomes released approximately 60% of the drug into PBS at pH 7.4 [41]. A literature article by Akita T et al. on Am80-loaded lipid nanoparticles (LNPs) for alveolar regeneration uses the same cationic lipid, Coatsome SS-OP, for triggered release [42]. For formulating the LNPs, the researchers used DOPE, DMG-PEG2000, cholesterol, and coatsome SS-OP. The lipids containing Am80 were solubilized in ethanol and injected into a malic acid buffer with 0.9% sodium chloride. The solvent was replaced by ultrafiltration. A release study was performed using 10 mM DTT as a reducing agent. The researchers observed an approximately 70% release within 20 hours [42]. We observed similar results with the release of MPI8-cSS-pegNL using 10 mM GSH as a reducing agent to break the disulfide bonds and release the entrapped drug.

An initial burst of drug release often occurs, wherein a significant percentage of the drug is released during the early stage of the release process. This result suggests that more encapsulation layers provide a denser matrix, offering greater protection against the dissolution of the active compound. These figures also support the validity of the Korsmeyer-Peppas model in describing the initial burst [43]. We applied the in vitro drug release profile to various mathematical models, presented the results graphically, and evaluated them using the correlation coefficient (r^2). The highest correlation coefficient indicates the mathematical model that best fits the drug release kinetics. For the release of MPI8 from MPI8-cSS-pegNLs, we determined that the Korsmeyer-Peppas model best described the in-vitro release, as it yielded the highest r2 ($r^2 = 0.995$).

Aerodynamic characterization of the MPI8-cSS-pegNLs

The particle size and morphology have a pronounced effect on all aspects of drug delivery to the lungs, including deposition, dissolution, and clearance mechanisms. Particles smaller than 4.7 µm can be distributed deep into the smaller airways, and this penetration correlates well with an excellent clinical response to local treatment. The alveoli are the target for the systemic delivery of drugs that are less efficient or less convenient when delivered by other routes. The respiratory deposition of particles follows four mechanisms: sedimentation, diffusion, impaction, and interception. Aerodynamic particle size distribution (APSD) data obtained from impactor studies provide information that helps predict the deposition of pharmaceutical aerodynamic particles in the lung and correlates with clinical responses in efficacy and safety studies of inhaled medications [44].

The formulation deposited at various stages is presented in the figure 8A. We presented the log plot of the effective cut-off diameter versus % drug deposition for each plate in Figure 9A. The MPI8-cSS-pegNLs showed an average MMAD of 4.40 ± 0.24 µm, a GSD of 2.02 ± 0.09, and an FPF of 37.88 ± 3.28 %, indicating deep drug delivery. In this case, we observe that a higher amount of drug is deposited in stages with a cut-off diameter of <4.7µm, indicating that

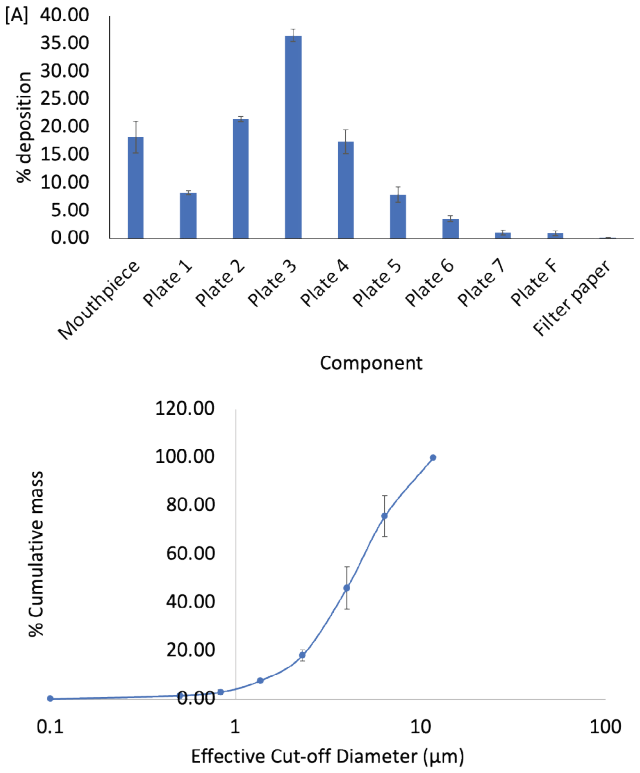


Figure 8: **[A]** Log plot of the effective cut-off diameter against % drug deposition on each plate and **[B]** Plot of log cumulative aerodynamic diameter (µm) versus the log of cumulative weight percent (%) of MPI8-cSS-pegNLs obtained from NGI after nebulization for 10 minutes and at a flow rate of 30 0.5 L/min, (n=3). We plotted the effective cut-off diameter as a logarithmic function. We used this to calculate the MMAD of the MPI8-cSS-pegNLs.

Kashikar R, et al., Arch Microbiol Immunology 2026
DOI:10.26502/ami.936500249

the formulation can reach the deep lung (Figure 8B). We observed that the highest amount of drug is deposited in stage 4, with an effective cut-off diameter of 2.3µm. Since stage 4 is associated with the secondary bronchi in the lung, we expect the formulation to deposit in the secondary bronchi of the deep lung. The geometric standard deviation (GSD) measures the variability of the particle diameters. A nebulized formulation with a GSD of <1.2 is described as monodisperse (uniform diameter distribution); an aerosol with a GSD >1.2 is described as polydisperse (heterogeneous particle distribution). GSD corresponds to 1 standard deviation in a 1-tailed standard normal distribution plot, and we obtained the percentage area under the curve from the table.

The p-value for z = -1 is 0.1587, and that for z = 1 is 0.8413. Therefore, ±1 standard deviation across the reading corresponds to 0.6862 (= 0.8413-0.1587). Similar to our results, Li et al. demonstrated that the nebulized amikacin-loaded nanoliposome (Arikace™) showed an MMAD of 3.6 ± 0.19µm and an FPF of 32.5% [9]. The majority (99.7%) of the nebulized Arikace™ was collected in ACI stages 0–5. With so little material deposited on stages 6 and 7 and on the filter, those fractions were considered irrelevant and were not evaluated [9]. Although material deposited on stages 0–5 was similar in terms of % associated amikacin, the material deposited onto stage 0 was statistically significantly different from that deposited on stages 1–5 in terms of L/D ratio (smaller) and liposome size (more significant)[9]. Stages 1–5 represented material expected to be respirable in droplet size (1.1 to 9 m), whereas the material collected in stage 0 described non-respirable droplets 9 m in diameter. Therefore, there appears to be no issue regarding the homogeneity of Arikace™ material and its expected distribution throughout the lung [9]. Li J et al. formulated a liposomal remdesivir inhalation comprising DPPC:cholesterol: DSPE-PEG2000, which was used at a 7:2:1 ratio for targeted lung delivery as a COVID-19 treatment [45]. Liposomes' aerodynamic characteristics, measured using the Copley Scientific NGI, showed an MMAD of 4.11 ± 0.104µm, a GSD of nearly 2, and a %FPF of around 50%. These results correlate very well with the results obtained in our study. An inhaled remdesivir nanoemulsion has been shown to effectively inhibit both wild-type and mutant SARS-CoV-2 by blocking viral binding to host cells and restricting intracellular replication[46]. The biocompatible, virucidal lipid nanoparticle comprising polyoxyethylene sorbitan oleate and sodium taurodeoxycholate mimics the properties of heparan sulfate proteoglycans and lipid rafts, demonstrating optimal physicochemical properties for pulmonary delivery, with minimal toxicity and a strong safety profile in vitro and in vivo[47]. It exhibits broad-spectrum virucidal activity, significantly reducing viral titers, including those of COVID-19, in multiple models by disrupting the viral envelope. In addition, a sustained-release inhaled Molnupiravir and peramivir co-loaded liposomal formulation, demonstrating favorable characteristics and nontoxicity in cell cultures[48]. An inhalable nano-in-microparticle system was developed by encapsulating Remdesivir in a polycaprolactone-based nanoparticle matrix, yielding high encapsulation efficiency and an optimal particle size for pulmonary delivery [49]. The formulation demonstrated good safety in Vero E6 cells and significantly reduced COVID-19 viral load at therapeutic concentrations. Spray-dried microparticles exhibited favorable aerodynamic properties and lung deposition.

Antiviral efficacy of the MPI8-cSS-pegNLs

The EC_{50} values of MPI8-cSS-pegNLs and MPI8 solution on Vero-E6-ACE2-TMPRSS2 cells in liquid culture were 1.2 and 1.1 micromolar, respectively, a difference that was not statistically significant (t-test, p = 0.16). This demonstrated the anti-viral activity of extended release MPI8-cSS-pegNLs treated for 48h and 72h against SARS-CoV-2, which was comparable to the drug solution (Figure 9 A-B). In another approach to intranasal delivery of nanoparticles against COVID-19, clofoctol-loaded Poly(lactic-co-glycolic acid) (PLGA)-based nanoparticles showed a high drug payload [50]. The pharmacokinetic evaluation demonstrated enhanced clofoctol bioavailability up to 8 hours following intranasal (i.n.) administration.

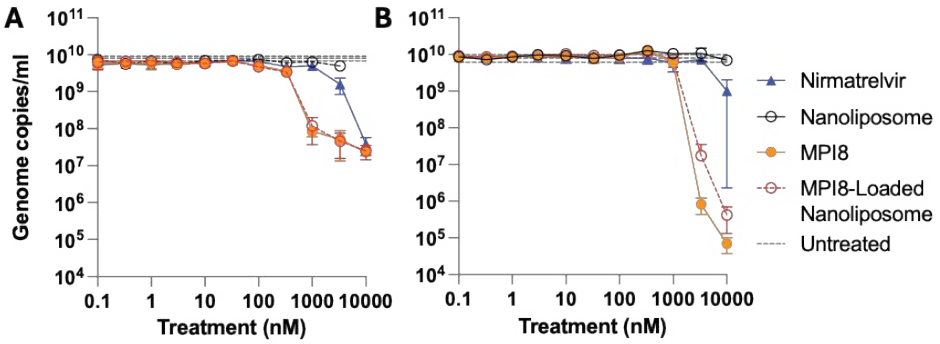


Figure 9: In vitro antiviral efficacy of MPI8-loaded nanoliposomes. Release of SARS-CoV-2 genomes from infected Vero-E6-ACE2-TMPRSS2 cells was measured 48h **(A)** or 72h **(B)** after inoculation.

Citation: Rama Kashikar, Shiqing Xu, Benjamin W Neuman, Wenshe Ray Liu, Pasupuleti Dedeepya,, Sathish Kumar, Mahavir Bhupal Chougule. Nebulized Extended-Release Cationic PEGylated Nanoliposomal Delivery of Antiviral dual inhibitor MPI8 for Targeting SARS-CoV-2 Infection. Archives of Microbiology and Immunology. 10 (2026): 156-169.

Kashikar R, et al., Arch Microbiol Immunology 2026
DOI:10.26502/ami.936500249

In preclinical models of COVID-19, including mice and hamsters, intranasal delivery of clofoctol-loaded nanoparticles resulted in a significant reduction in pulmonary viral load. We anticipate that the in vivo efficacy will be superior to that of the drug solution due to distinct lung clearance, distribution, and metabolism. The developed nebulized MPI8-cSS-pegNLs had characteristics consistent with the target profile. The nebulized extended-release MPI8-cSS-pegNLs demonstrated promising potential for the treatment of COVID-19.

Conclusion

We formulated MPI8-loaded PEGylated nanoliposomes using cationic lipids with an average particle size of 292.5±6.6 nm, meeting the target range of less than 250 nm during extrusion. The final particle size after extrusion was 180.5±2.6 nm. The extrusion process did not have a detrimental effect on the polydispersity index, which was 0.144±0.028, while the zeta potential was 0.597±0.038 mV. The extrusion process had a significant effect on the % entrapment efficiency of the drug, which increased from 60.773±2.681 % w/v to 95.479±1.842 % w/v. However, it had no significant effect on % drug loading and % assay, which were 62.170±0.741 % w/w and 100±0.236 % w/v, respectively. We successfully formulated MPI8-cSS-pegNLs, which showed extended release of up to 12 hours in SLF solution, enabling a twice-daily dosing regimen. MPI8-CSS-PEGNLs released 104.084±1.836% in 12 hours. Based on the correlation coefficient computed using the release kinetics software DDSolver, the MPI8-cSS-pegNLs follow a Korsmeyer-Peppas release model (r^2 = 0.995). The MPI8-cSS-pegNLs, upon nebulization, showed an MMAD of 4.40 ± 0.24 µm, a GSD of 2.02 ± 0.09, and an FPF of 37.88% ± 3.28, thereby indicating deep-lung delivery, which is essential for the treatment of COVID-19. The MPI8-cSS-pegNLs treated for 48 h and 73 h exhibited antiviral activity against SARS-CoV and showed high potential as a new therapy for managing SARS-CoV-2 infection.

Acknowledgments

The authors thank Mercer University and Texas A&M for providing study facilities. Dr. Chougule would like to acknowledge partial support from the National Heart, Lung, and Blood Institute of the National Institutes of Health, award R15HL138718. The authors acknowledge the financial support provided by NIH (Grant R35GM145351 to W.R.L.), Welch Foundation (Grants A-1715 to W.R.L. and A-2174 to S.X.), and the Texas A&M Advancing Discovery to Market Program.

Conflicts of Interest must be explicitly declared.

Dr. Chougule is affiliated with Adexp BioPharma Product Consulting, Litigation and Patent Expert LLC. There are no further conflicts of interest to declare.

CRediT Contributor Role Authorship Statement

Participated in research design: Kashikar Rama, Xu Shiqing, Liu Wenshe Ray, and Chougule Mahavir.

Conducted experiments: Kashikar Rama, Pasupuleti Dedeepya.

Performed data analysis: Kashikar Rama.

Wrote or contributed to the writing of the manuscript: Kashikar Rama, Chougule Mahavir.

References

1. Cdcgov, *How Coronavirus Spreads | CDC* (2022).
2. Cdcgov, *How to Protect Yourself and Others | CDC* (2023).
3. Olebo DF and MC Igwe. *Comparative analysis of virology and pathogenesis of SARS-CoV-2 and HIV infections: Implications for public health and treatment strategies.* Infection and drug resistance (2025): 269-283.
4. Maglione MA, et al. *A rapid systematic review of US Food and Drug Administration-authorized COVID-19 treatments*. in *Open Forum Infectious Diseases* (2025).
5. Sullivan DJ, et al. *A Rapid Systematic Review of US Food and Drug Administration–authorized COVID-19 Treatments*. in *Open Forum Infectious Diseases* (2025).
6. Sharma L, et al. *Therapeutic Approaches to Treat SARS-CoV-2.* ChemMedChem 21 (2026): e202500387.
7. Yoshimura A and VV Zhdankin. *Recent Progress in Synthetic Applications of Hypervalent Iodine(III) Reagents.* Chemical Reviews 124 (2024): 11108-11186.
8. Aadil KR, et al. *Nanotechnology assisted strategies to tackle COVID and long-COVID.* Bionanoscience 15 (2025): 217.
9. Li Z, et al. *Characterization of nebulized liposomal amikacin (Arikace) as a function of droplet size.* J Aerosol Med Pulm Drug Deliv 21 (2008): 245-54.
10. Alves MC, et al. *Therapeutic approaches for COVID-19: A review of antiviral treatments, immunotherapies, and emerging interventions.* Advances in Therapy 42 (2025): 3045-3058.
11. Harrison C. *Coronavirus puts drug repurposing on the fast track.* Nat Biotechnol 38 (2020): 379-381.
12. El Zawily A, et al. *Comprehensive review on COVID-19: etiology, pathogenicity, and treatment.* Frontiers in Medicine 12 (2025): 1569013.
13. Surnar B, et al. *Clinically approved antiviral drug in an orally administrable nanoparticle for COVID-19.* ACS

Kashikar R, et al., Arch Microbiol Immunology 2026
DOI:10.26502/ami.936500249

pharmacology & translational science 3 (2020): 1371-1380.

14. Fan Y, et al. *Advances in inhaled nanoparticle drug delivery for pulmonary disease management.* The FASEB Journal 39 (2025): e71191.

15. Shah KA, et al. *Current trends in inhaled pharmaceuticals: challenges and opportunities in respiratory infections treatment.* Journal of Pharmaceutical Investigation 55 (2025): 191-225.

16. Rana D, et al. *Recent advances in antiviral drug delivery strategies.* AAPS PharmSciTech 26 (2025): 73.

17. Ali T. *Nanomedicine approaches to overcome barriers in pulmonary drug delivery for respiratory diseases.* Current Pharmaceutical Research (2025): 30-44.

18. Kashikar R, et al. *Formulation and In-Vitro Testing of Nebulized Camostat Mesylate Loaded Nanoliposomes for the Treatment of SARS-CoV-2 Infection.* AAPS PharmSciTech 26 (2025): 139.

19. Kashikar R, et al. *Design of experiments using box behnken design in the development, characterization, mathematical modeling, and evaluation of lung targeted nebulized antiviral camostat mesylate loaded pegylated nanosuspension product.* Journal of Drug Delivery Science and Technology 98 (2024): 105810.

20. Ma XR, et al. *MPI8 is Potent against SARS-CoV-2 by Inhibiting Dually and Selectively the SARS-CoV-2 Main Protease and the Host Cathepsin L.* ChemMedChem 17 (2022): e202100456.

21. Wang Y, et al. *Accurate Mass Identification of an Interfering Water Adduct and Strategies in Development and Validation of an LC-MS/MS Method for Quantification of MPI8, a Potent SARS-CoV-2 Main Protease Inhibitor, in Rat Plasma in Pharmacokinetic Studies.* Pharmaceuticals (Basel) 15 (2022).

22. *601 AEROSOLS, NASAL SPRAYS, METERED-DOSE INHALERS, AND DRY POWDER INHALERS* (2023).

23. Hald Albertsen C, et al. *The role of lipid components in lipid nanoparticles for vaccines and gene therapy.* Adv Drug Deliv Rev 188 (2022): 114416.

24. Gouda A, et al. *Ethanol injection technique for liposomes formulation: An insight into development, influencing factors, challenges and applications.* Journal of Drug Delivery Science and Technology 61 (2021): 102174.

25. de Barros AOdS, et al. *Polymeric nanoparticles and nanomicelles of hydroxychloroquine co-loaded with azithromycin potentiate anti-SARS-CoV-2 effect.* Journal of nanostructure in chemistry 13 (2023): 263-281.

26. Li J, et al. *Design of MERS-CoV entry inhibitory short peptides based on helix-stabilizing strategies.* Bioorganic & Medicinal Chemistry Letters 97 (2024): 129569.

27. Medhi R, et al. *Nanoparticle-based strategies to combat COVID-19.* ACS Applied Nano Materials 3 (2020): 8557-8580.

28. Qin T, et al. *Catalytic inactivation of influenza virus by iron oxide nanozyme.* Theranostics 9 (2019): 6920.

29. Hanafy NAN and MA El-Kemary. *Silymarin/curcumin loaded albumin nanoparticles coated by chitosan as muco-inhalable delivery system observing anti-inflammatory and anti COVID-19 characterizations in oleic acid triggered lung injury and in vitro COVID-19 experiment.* Int J Biol Macromol 198 (2022): 101-110.

30. Namiot ED, et al. *Nanoparticles in clinical trials: analysis of clinical trials, FDA approvals and use for COVID-19 vaccines.* International journal of molecular sciences 24 (2023): 787.

31. Wilson B and KM Geetha. *Lipid nanoparticles in the development of mRNA vaccines for COVID-19.* Journal of drug delivery science and technology 74 (2022): 103553.

32. Sommer AP, et al. *Pulmonary and intranasal delivery of thymoquinone-loaded nanoparticles for Mucormycosis & Covid-19.* Precis Nanomed 4 (2021): 795-800.

33. Sebaaly C, S Haydar and H Greige-Gerges. *Eugenol encapsulation into conventional liposomes and chitosan-coated liposomes: A comparative study.* Journal of Drug Delivery Science and Technology 67 (2022): 102942.

34. Danaei M, et al. *Impact of Particle Size and Polydispersity Index on the Clinical Applications of Lipidic Nanocarrier Systems.* Pharmaceutics 10 (2018).

35. Duong TT, et al. *Nanoformulation and Evaluation of Oral Berberine-Loaded Liposomes.* Molecules 26 (2021).

36. Smith MC, et al. *Zeta potential: a case study of cationic, anionic, and neutral liposomes.* Analytical and Bioanalytical Chemistry 409 (2017): 5779-5787.

37. Akita T, et al. *Am80-Encapsulated Lipid Nanoparticles, Developed with the Aim of Achieving Alveolar Regeneration, Have an Improvement Effect on Pulmonary Emphysema.* Pharmaceutics 15 (2022).

38. Jaafar-Maalej C, et al. *Ethanol injection method for hydrophilic and lipophilic drug-loaded liposome preparation.* Journal of Liposome Research 20 (2010): 228-243.

39. Sarfraz M, et al. *Development of Dual Drug Loaded Nanosized Liposomal Formulation by A Reengineered*

Kashikar R, et al., Arch Microbiol Immunology 2026
DOI:10.26502/ami.936500249

Ethanolic Injection Method and Its Pre-Clinical Pharmacokinetic Studies. Pharmaceutics 10 (2018).

40. Weng J, HHY Tong, and SF Chow. *In Vitro Release Study of the Polymeric Drug Nanoparticles: Development and Validation of a Novel Method.* Pharmaceutics 12 (2020).
41. Taherzadeh S, et al. *Preparation, Statistical Optimization and Characterization of Propolis-Loaded Solid Lipid Nanoparticles Using Box-Behnken Design.* Adv Pharm Bull 11 (2021): 301-310.
42. Akita T, et al. *Intracellular Drug Delivery Process of Am80-Encapsulated Lipid Nanoparticles Aiming for Alveolar Regeneration.* Pharmaceuticals 16 (2023): 838.
43. Janssen MJH, et al. *Doxorubicin decomposition on storage. Effect of pH, type of buffer and liposome encapsulation.* International Journal of Pharmaceutics 23 (1985): 1-11.
44. Newman SP and HK Chan. *In vitro-in vivo correlations (IVIVCs) of deposition for drugs given by oral inhalation.* Adv Drug Deliv Rev 167 (2020): 135-147.
45. Li J, et al. *Liposomal remdesivir inhalation solution for targeted lung delivery as a novel therapeutic approach for COVID-19.* Asian J Pharm Sci 16 (2021): 772-783.
46. Wang H, et al. *ACE2 Receptor-Targeted Inhaled Nanoemulsions Inhibit SARS-CoV-2 and Attenuate Inflammatory Responses.* Advanced Materials 36 (2024): 2311537.
47. Martins YA, et al. *Novel Wide-Spectrum Virucidal Lipid Nanoparticles.* Small 22 (2026): e07669.
48. Keskin H, et al. *Development of molnupiravir and peramivir loaded liposome formulations for combined antiviral therapy.* Pharmaceutical development and technology 30 (2025): 691-711.
49. Sani ATM, et al. *Polymeric nano-in-microparticles for pulmonary delivery of remdesivir against SARS-CoV-2.* RSC Pharmaceutics 3 (2026): 552-563.
50. Bolduc M, et al. *PapMV nanoparticles: A novel pathway to SARS-CoV-2 protection, distinct from Imidazoquinolines.* Nanomedicine: Nanotechnology, Biology and Medicine (2025): 102887.

This article is an open access article distributed under the terms and conditions of the Creative Commons Attribution (CC-BY) license 4.0

Citation: Rama Kashikar, Shiqing Xu, Benjamin W Neuman, Wenshe Ray Liu, Pasupuleti Dedeepya,, Sathish Kumar, Mahavir Bhupal Chougule. Nebulized Extended-Release Cationic PEGylated Nanoliposomal Delivery of Antiviral dual inhibitor MPI8 for Targeting SARS-CoV-2 Infection. Archives of Microbiology and Immunology. 10 (2026): 156-169.